metals

MDPI

Article

Tailoring Interfacial Bonding and Tensile Properties in Cu/Al/Cu Laminated Composites by Adjusting Thickness Ratio

Wenbo Bai [1], Mahmoud Ebrahimi [2], Huisheng Cai [1,3], Yuchao Zhao [1,4], Nannan Zhang [1] and Qudong Wang [1,*]

[1] National Engineering Research Center of Light Alloy Net Forming and Key State Laboratory of Metal Matrix Composites, School of Material Science and Engineering, Shanghai Jiao Tong University, Shanghai 200240, China; bwbysu@126.com (W.B.); caihuisheng@imut.edu.cn (H.C.); zyqzhaoyuchao@163.com (Y.Z.); jszhangnan@126.com (N.Z.)

[2] Department of Mechanical Engineering, Faculty of Engineering, University of Maragheh, Maragheh 83111-55181, Iran; ebrahimi@maragheh.ac.ir

[3] Inner Mongolia Key Laboratory of New Materials and Surface Engineering, School of Material Science and Engineering, Inner Mongolia University of Technology, Hohhot 010051, China

[4] School of Intelligent Manufacturing Engineering, Shanghai College of Science & Technology, Shanghai 201899, China

* Correspondence: wangqudong@sjtu.edu.cn

Abstract

The design of the overall thickness and thickness ratio in multilayered composites is vital because it affects interfacial microstructures and mechanical properties. These elements are significant in the application of multilayered composites in diverse scenarios. This study systematically investigated the interfacial microstructure, mechanical properties, and fracture mechanisms of Cu/Al/Cu trilayered composites with varying overall thicknesses and copper thickness ratios. The microstructure results showed that the distribution and thickness of intermetallic compounds (IMCs) at the Cu/Al interface changed significantly with different thickness designs. As the Cu thickness ratio increased from 20% to 35%, the intermetallic layer transitioned from a continuous structure to a fragmented one in both the 1 mm and 2 mm composites. Additionally, the bonding mechanism evolved from primarily metallurgical bonding to a combination of metallurgical and mechanical bonding. In the 4 mm composite with a 35% Cu thickness ratio, the interfacial intermetallic layer comprised three sublayers identified as Al_4Cu_9, AlCu, and Al_2Cu. Tensile results indicated that increasing the Cu thickness ratio markedly enhanced strength and ductility: the 1 mm composite showed increases of 22.3% in ultimate tensile strength and 70.9% in elongation, while the 2 mm composite exhibited increases of 32.4% and 38.7%, respectively. In contrast, increasing the overall thickness had only a limited effect. Fractography revealed ductile fracture features in both the Al and Cu layers, characterized by more compact interfaces, deeper dimples, and more pronounced tear ridges at higher Cu thickness ratios. These findings demonstrate that optimizing the Cu thickness ratio is an effective strategy for enhancing interfacial bonding strength and overall mechanical performance in Cu/Al/Cu composites.

Keywords: interfacial microstructure; intermetallic compounds; mechanical bonding; metallurgical bonding; mechanical properties; fractography

Check for updates

Academic Editor: Jürgen Eckert

Received: 19 May 2026
Revised: 11 June 2026
Accepted: 12 June 2026
Published: 14 June 2026

Copyright: © 2026 by the authors. Licensee MDPI, Basel, Switzerland. This article is an open access article distributed under the terms and conditions of the Creative Commons Attribution (CC BY) license.

1. Introduction

Recently, Cu/Al laminated metallic composites (LMCs) have attracted much attention in both academic and industrial sectors due to their cost-effectiveness [1–4], corrosion resistance, lightweight property [5], excellent electric conductivity, prominent thermal

dissipation performance, and suitable formability [6]. Through years of dedicated research and persistent efforts, Cu/Al LMCs have found broad applications in various areas of human society, including thermal dissipation substrate material, the electronics industry, the automotive sector, renewable energy fields, and aerospace [7–9].

To achieve various structures and optimal mechanical properties, most Cu/Al LMCs are fabricated using solid-state techniques [10,11]. In this regard, the main solid-state processing methods include explosive welding [12], diffusion bonding [13,14], extrusion [15], vacuum hot pressing [16], friction-stir welding [17,18], accumulative roll bonding [19], and roll bonding [20]. Among them, roll bonding is particularly favored in the industrial fabrication of Cu/Al composites due to its high efficiency, low cost, concise process, and consistent product quality. However, during the rolling process of Cu/Al composites, the dissimilar layers with varying properties often demonstrate different deformation capacities [21]. This discrepancy leads to intense, incoherent deformation, which adversely affects their performance. Consequently, extensive research has indicated that the sample size and thickness ratio of LMCs are crucial factors influencing the behavior of composite deformation, the mode of interface fracture, and the overall mechanical properties [22–25].

Li et al. [26] demonstrated that the impact energy and crack initiation energy of heterogeneous titanium laminated composites are significantly influenced by the thickness ratios of the titanium layers, a relationship explained by the various types of interface grain orientations. Lei et al. [27] prepared Mg/Al LMCs with magnesium thickness ratios of 2:1, 3:1, and 5:1. Considering the effect of interface microstructure evolution on mechanical properties, the 5:1 Mg thickness ratio exhibited more coordinated deformation behavior and the lowest interface defect density. Atifeh et al. [28] investigated the microstructure and formability of Al/steel bilayer sheets with varying initial thicknesses and thickness ratios. They observed changes in interface grain size and the formation of shear bands at different thickness ratios. The optimized parameters for the bilayer sheet were determined as 4 mm for the aluminum thickness, 0.8 mm for the steel thickness, and a 45% reduction in thickness. Additionally, temperature is an important factor that interacts with the thickness ratio to influence the mechanical properties of composites. In this regard, Chen et al. [29] studied the morphology and bonding properties of aluminum/steel clad plates at varying thickness ratios and rolling temperatures. Their findings indicated that the interface shear strength depends on the initial thickness ratio, except when the rolling temperature reaches 600 °C. Furthermore, fracture behavior was also impacted by the thickness ratio. In research conducted by Xia et al. [30], it was observed that as the aluminum thickness ratio increased, the tolerance for premature interfacial microcracks also improved, leading to more uniform crack distributions on the fracture surface. The varying bonding behaviors and fracture modes resulted in different distributions of interface stress and strain across the distinct thickness ratios. Wang et al. [31] conducted both experimental and numerical studies on the coordinated deformation behavior at the interface of Cu/Al composites with varying thickness ratios. The findings indicated that the distribution of interface normal stress initially becomes uniform; however, as the copper thickness ratio increases, it becomes less uniform. Notably, the bonding force for the 8:4 Cu/Al thickness ratio was approximately 174% greater than that of the 4:8 ratio. The importance of the thickness ratio in deformation coordination between different constituent layers and its impact on the overall properties of multilayered metallic composites has been demonstrated in numerous studies [32–35]. While significant research has addressed the effects of thickness ratios on LMCs during fabrication, there is a notable lack of studies investigating the mechanical properties and interface microstructure of rolled Cu/Al/Cu composites with varying overall thicknesses and thickness ratios.

Cu/Al/Cu trilayered composites have emerged as an ideal alternative to traditional copper and aluminum plates. These special trilayer composites combine the best features of both materials, providing the excellent conductivity of copper and the light weight of aluminum [36–38]. As a result, various industries, including aerospace, automotive, and construction, widely use Cu/Al/Cu trilayered composites in power transmission equipment [39–41]. In this paper, Cu/Al/Cu trilayered composites with different overall thicknesses and copper thickness ratios were fabricated by high-temperature oxygen-free rolling. The effects of overall composite thickness and thickness ratio on the interface microstructure were investigated. Additionally, the deformation behavior and fracture mechanisms of Cu/Al/Cu composites under varying thickness ratios were analyzed through uniaxial tensile testing and fracture morphology characterization. This work aimed to develop a practical design strategy for regulating the interface microstructure and mechanical properties of Cu/Al/Cu trilayered metallic composites, thereby promoting better practical applications of Cu/Al/Cu LMCs.

2. Materials and Methods

2.1. Materials

In this study, Cu/Al/Cu trilayer composites were prepared using high-temperature oxygen-free rolling to achieve oxide-free metallurgical bonding and to control the evolution of the interfacial microstructure. The base and cladding layers of the Cu/Al/Cu composites consisted of commercially pure copper and commercial pure 1060 aluminum (Al1060), respectively. Table 1 lists the detailed chemical compositions of the copper and aluminum samples.

Table 1. Chemical composition of copper and aluminum used for the fabrication of Cu/Al/Cu trilayered composites.

	Cu	Al	Fe	Cr	Si
Pure Cu	Bal.	-	0.003%	-	0.003%
Al1060	0.030%	Bal.	0.260%	0.150–0.350%	-

The Cu/Al/Cu composites with varying Cu thickness ratios were supplied by JiangsuZhongse composite material Co., Ltd., Wuxi, China. The detailed fabrication process of the Cu/Al/Cu composite is outlined as follows: The optimized Cu/Al1060 bilayer composite material was selected for this procedure [42]. Initially, these bilayer composite materials underwent two rolling passes, followed by annealing at 350 °C for 2 h. This process resulted in two types of composites, each 4 mm thick, featuring Cu layer proportions of 10% and 17.5%. Following this, the Al side was polished to remove surface oxides and then preheated in a substrate heating furnace prior to rolling. The rolling process was performed using a rolling mill operating at a linear speed of 3 m/min, with a work roll diameter of 350 mm and a rolling temperature of 250 °C. After completing 1 to 3 rolling passes, the thickness of the Cu/Al1060/Cu trilayer composite was reduced to 4 mm, 2 mm, and 1 mm, respectively, while the proportions of each Cu layer remained approximately 10% and 17.5%. Finally, using the optimized annealing parameters established for the Cu/Al1060 bilayer composite, the high-temperature oxygen-free rolled Cu/Al1060/Cu trilayer composite was annealed at 350 °C for 2 h. This study utilized five symmetric Cu/Al/Cu trilayered composites, each with distinct Cu thickness ratios. Detailed thickness values are provided in Table 2, where the thickness ratio denotes the combined thickness of the two copper layers, which are identical on both the top and bottom sides of the Cu/Al/Cu trilayered composite. For instance, the designation “1-20” indicates a 1 mm Cu/Al/Cu composite with a thickness ratio of 10:80:10.

Table 2. Five Cu/Al/Cu trilayered composites with different copper thickness ratios used in this study.

Composite Designation	Overall Thickness (mm)	Cu Thickness Ratio (%)
"1-20"	1	20
"1-35"	1	35
"2-20"	2	20
"2-35"	2	35
"4-35"	4	35

2.2. Microstructural Characterization and Mechanical Properties

Samples for microstructural characterization were prepared using electrical discharge machining (Sodick Co., Ltd., Yokohama, Japan). Following this, a series of mechanical grinding steps was performed on the RD/TD planes of the samples, utilizing P400, P800, P1200, P2000, P5000, and P7000 SiC abrasive papers. This was succeeded by polishing with 0.05 µm colloidal silica to eliminate grinding scratches and achieve a mirror-like finish. Ultimately, microstructural analyses and interfacial characterizations were carried out using a Zeiss Sigma 500 scanning electron microscope (Thermo Fisher Scientific, distributed by Phenom Scientific Instrumen Co., Ltd., Shanghai, China) that was equipped with a backscattered electron (BSE) detector and integrated energy dispersive X-ray spectroscopy (EDS). The SEM operated at an accelerating voltage of 20 kV. In this regard, examinations such as elemental mapping, line scanning, and point analysis were employed to clarify interfacial diffusion profiles, identify phases, and assess micro-segregation [43].

To investigate the effect of composite thickness and the copper thickness ratio on the mechanical properties of Cu/Al/Cu LMCs, a uniaxial tensile test was conducted. Tensile samples were prepared along the rolling direction (RD) with an overall length of 110 mm, a width of 10 mm, and a gauge length of 50 mm. Before testing, the samples were mechanically ground using P600 abrasive paper (Starcke GmbH & Co. KG, Melle, Germany). The tensile tests were performed on an MTS C45.105 machine at a strain rate of 1×10^{-3} s^{-1} at room temperature, with strain measured using a video extensometer (Instron, AVE3, Norwood, MA, USA). At least three specimens were tested for each temperature sample to ensure the reproducibility of the data. Fractography was also carried out through SEM in order to investigate the fracture mechanisms. Dimensional specifications of sample preparation for tensile tests and microstructure analyses were shown schematically in Figure 1.

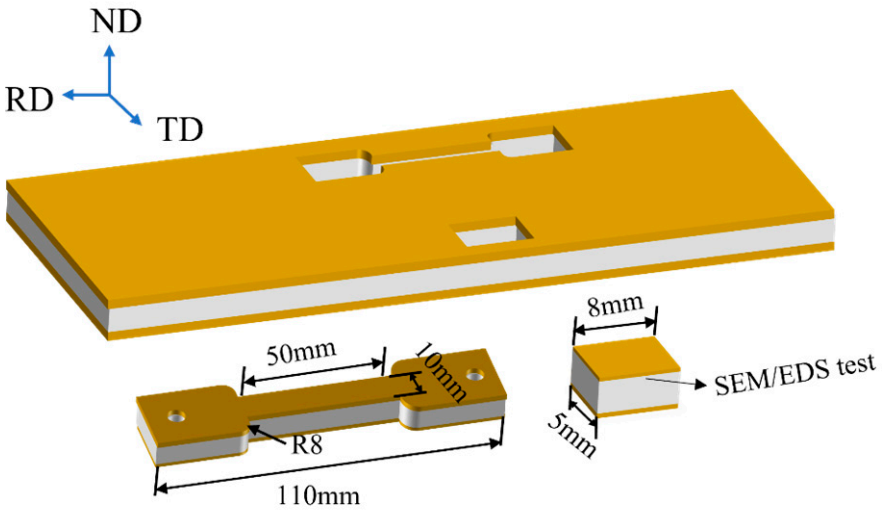


Figure 1. Schematic representation of the prepared samples for the tensile test and microstructure analysis.

3. Results and Discussion

3.1. Interface Analysis

Figure 2 represents the micrograph of the ND-RD section of Cu/Al/Cu trilayered composites which have varying thicknesses and copper thickness ratios. Accordingly, a distinct thickness ratio profile was evident in the micrographs. Additionally, a continuous and straight bonding interface was observed, with no cracks present in the joint interfaces.

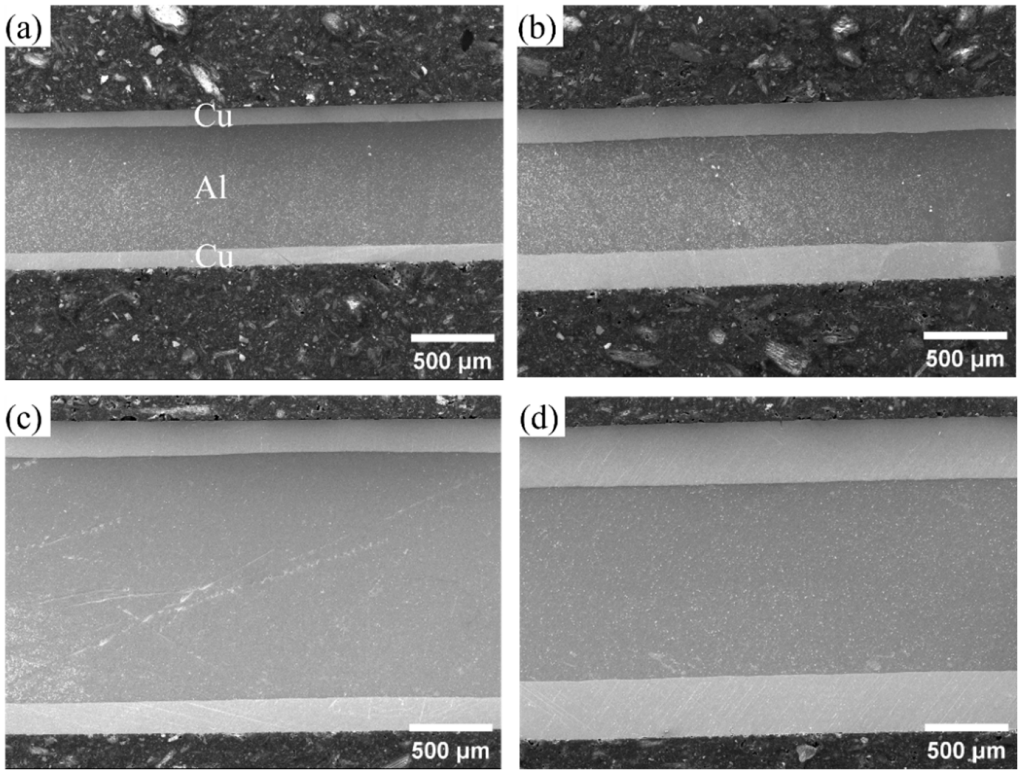


Figure 2. Observation of Cu/Al/Cu trilayered metallic composites at the RD-ND section, fabricated at varying thickness ratios: (**a**) "1-20", (**b**) "1-35", (**c**) "2-20", and (**d**) "2-35".

Figure 3 illustrates the results of SEM observations and EDS analysis of the Cu/Al interface with varying overall thicknesses and copper thickness ratios. In this regard, EDS line scan profiles are shown in Figure 3(a4,b4,c4,d4,e4), with yellow arrow symbols positioned perpendicular to the interface to provide better insight into the interfacial elemental distribution. In Figure 3(a1–a4), a layer with distinct contrast is observed at the Cu/Al interface, identified as the intermetallic composites (IMCs). The EDS mapping results indicate that Cu and Al atoms undergo mutual diffusion, resulting in a straight, uniform diffusion layer. Furthermore, the line scanning curves at the interface become approximately horizontal within the diffusion layer, suggesting a sudden change in element content due to the formation of intermetallic compounds. These findings align with previous studies [44,45], which indicate that IMCs typically form at the Cu/Al interface and significantly affect the properties of the composite material. To determine the thickness of the IMCs for each of the five composites, 25 equidistant measurements were taken at 0.5 µm intervals using ImageJ software (1.54s 26 March 2026). Interface area fraction was also measured using ImageJ by calculating the IMC length fraction along the interface. In the case of the 1 mm Cu/Al/Cu composite with a 20% Cu thickness ratio ("1-20"), the IMC layer exhibits a primarily continuous distribution, with a 3.41 µm thickness and an interface area fraction of 94%. Some cracks are also noted within the IMC layer, suggesting that the bonding mechanism for the "1-20" Cu/Al/Cu composite is predominantly metal-

lurgical bonding. In contrast, the "1-35" Cu/Al/Cu composite displays a distinct interface microstructure (Figure 3(b1)), characterized by alternating regions of IMCs and IMC-free areas. In the separation area of the primary IMC layer, the Cu and Al layers appear to be extruded and filled. The thickness of the IMCs in this case is 2.17 μm, which is significantly lower than the "1-20" composite. The interface area fraction was 68%, which is higher than that of the "1-20" composite. These variations in interface structure and IMC distribution result in differing mechanical properties, which will be discussed later. Moreover, as shown in Figure 3(b2–b4), the EDS mapping results for the 1 mm 35–Cu-ratio ("1-35") composite display a more irregular diffusion layer compared to the 1 mm 20–Cu-ratio ("1-20") counterpart. This segregated structure of the intermetallic compounds is expected to introduce additional mechanical bonding strength under shear loading, as reported in extensive studies [46–48]. Consequently, the bonding mechanism for the "1-35" composite was determined to be a combination of metallurgical and mechanical bonding. Figure 3(c1) illustrates the interface microstructure of the "2-20" Cu/Al/Cu composite, which have an IMC thickness of 3.36 μm and IMC interface area fraction of 96%. It is noteworthy that numerous cracks have developed in the IMC layer near the Al layer; however, the overall IMC layer remains largely continuous. As shown in Figure 3(d1), the thickness of the IMCs at the interface of the "2-35" Cu/Al/Cu composite was measured to be 3.01 μm, with an interface area fraction of 84%. The IMC layer is more severely fragmented compared to the "2-20" condition, indicating a preliminary trend toward mechanical bonding formation. This is because a greater rolling force is required for Cu/Al/Cu composites with a higher Cu thickness ratio during the rolling process, which slightly thins the IMCs and causes them to break. Particularly, at the interface of the 4 mm 35–Cu-ratio Cu/Al/Cu composite, as depicted in Figure 3(e1), an intermittent IMC layer is present. The IMC thickness was recorded at 3.12 μm, and the gaps between adjacent IMCs along the rolling direction have increased compared to the "1-35" counterpart, suggesting enhanced mechanical bonding behavior.

The thickness and distribution of intermetallic compounds are crucial to the mechanical properties of fabricated composites. Deng et al. [49] observed varying distributions of interface IMCs in Al/Fe composites due to different heat treatments. Their findings indicated that granular IMCs shifted the maximum shear stress location from the interface to the aluminum layer, thereby enhancing the bonding strength. Zhang et al. [50] utilized electric current to induce different IMC formations in the Al/steel interface, effectively regulating its interfacial bonding strength. Qiu et al. [47] illustrated that the aluminum layer's penetration into the gaps of IMCs in Al/steel composites facilitated additional mechanical bonding. Cai et al. [51] also reported distinct shear properties associated with various IMC distributions in the Cu/Al interface. In this regard, the fragments of the IMC layer remaining at the interface of Cu/Al/Cu composites with a higher copper ratio can act as particulate pinning sites under shear stress, further strengthening the interface. The presence of scattered IMCs at the interface signifies robust mechanical bonding, complemented by diffusion bonding in the composite structure. As previously described, there is a notable difference in the interface microstructure between Cu/Al/Cu composites with varying thicknesses and copper thickness ratios. In Cu/Al/Cu trilayer composites, the IMC layer exhibits a greater tendency to fracture, and the IMC thickness decreases slightly as the copper thickness ratio increases from 20% to 35%. This suggests a shift in the bonding mechanism from purely metallurgical bonding to a combination of metallurgical and mechanical bonding. Furthermore, increasing the overall composite thickness results in a larger gap between adjacent IMC fragments, which enhances the contact area between the aluminum and copper layers. Additionally, the IMC thickness experiences a slight increase. Such discrepancies in microstructure account for the differing mechanical properties of

Cu/Al/Cu composites with varying overall thicknesses and copper thickness ratios, which will be further elaborated upon in the subsequent discussion.

According to Figure 4, it is obvious that the interface IMC layer is clearly composed of three distinct sublayers (I, II, and III), which were differentiated by varying light and shade conditions. In this regard, in order to investigate the composition of these three IMC sublayers, an EDS point scanning test was conducted on the interface of the 4 mm 35–Cu thickness-ratio ("4-35") composite. The results are represented in Table 3. Based on the obtained results and relevant research papers [38–40] on the constituents of IMCs in the interfaces of Cu/Al laminated composites, it can be confirmed that layers I, II, and III correspond to Al_4Cu_9, AlCu, and Al_2Cu, respectively.

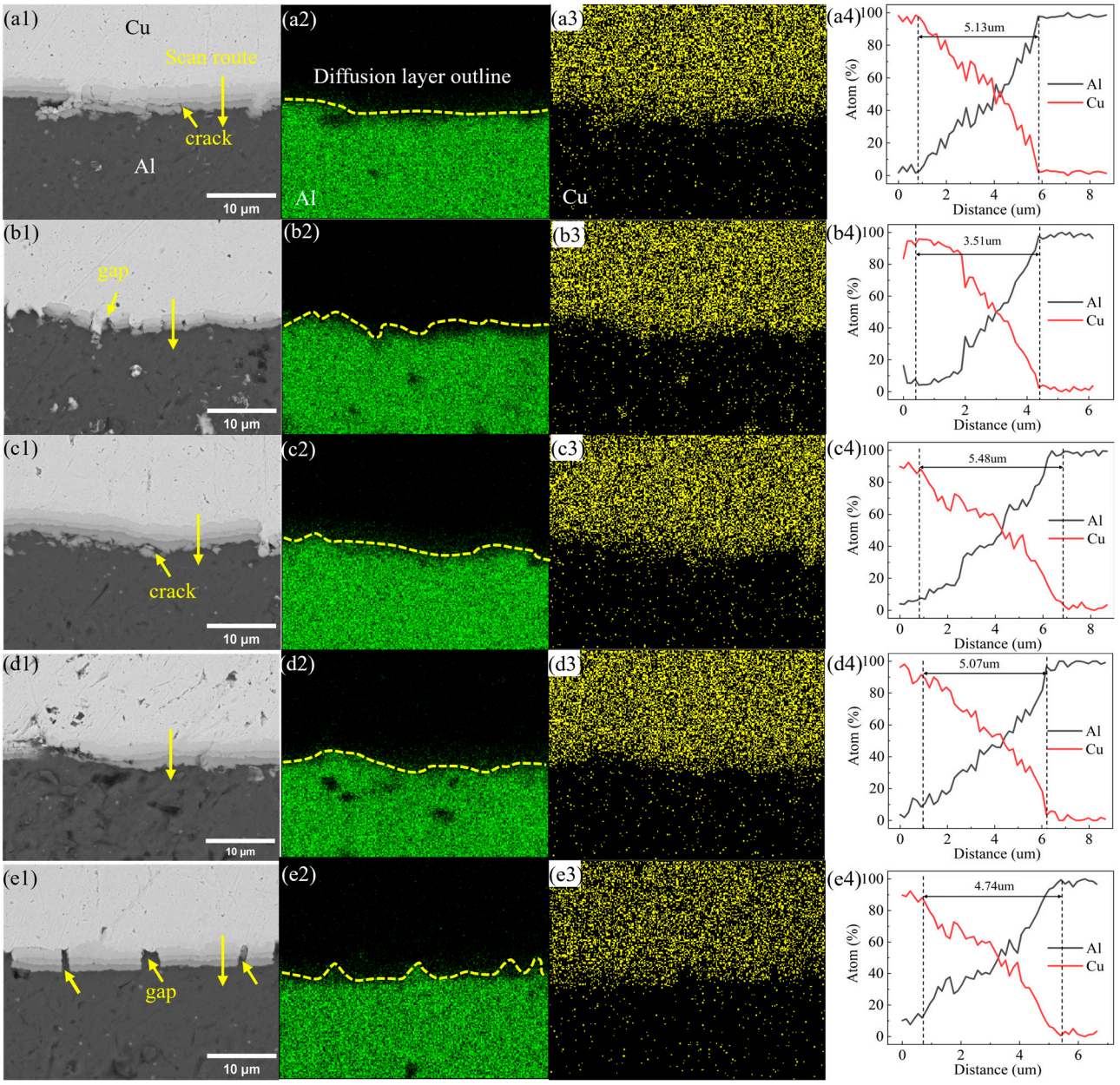


Figure 3. SEM observation, EDS line scanning, and elemental mapping of the Cu/Al interface in the fabricated Cu/Al/Cu trilayered composites: (**a1**–**a4**) 1 mm 20–Cu-thickness-ratio, labeled "1-20", (**b1**–**b4**) 1 mm 35–Cu-thickness-ratio, labeled "1-35", (**c1**–**c4**) 2 mm 20–Cu-thickness-ratio, labeled "2-20", (**d1**–**d4**) 2 mm 35–Cu-thickness-ratio, labeled "2-35", (**e1**–**e4**) 4 mm 35–Cu-thickness-ratio, labeled "4-35". Note that dashed lines indicate the thickness of the diffusion layer.

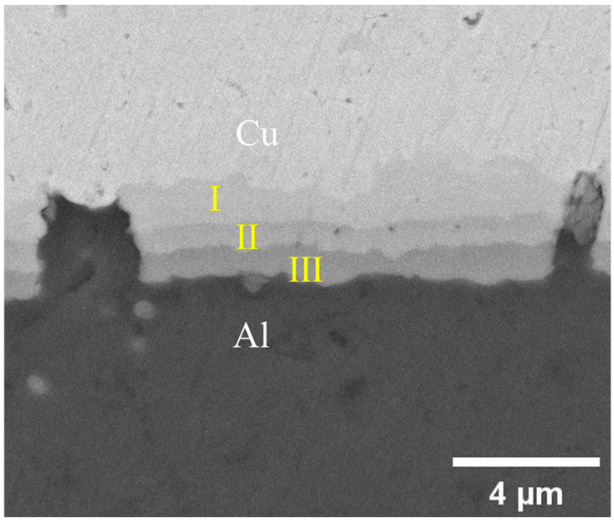


Figure 4. Three sublayers of the intermetallic compounds (denoted by I, II, and III) at the interface of 4 mm 35–Cu-thickness-ratio ("4-35") Cu/Al/Cu composites.

Table 3. The point EDS results of IMCS (at.%) at the interface of 4 mm 35–Cu-thickness-ratio ("4-35") Cu/Al/Cu composites, as shown in Figure 4.

IMCs	Element	Atomic (%)	Average Atomic (%)	Possible Phase
I	Al	35.13 36.27 34.68	35.36	Al_4Cu_9
	Cu	59.11 63.53 60.32	61.65	
II	Al	47.96 50.46 48.86	49.09	AlCu
	Cu	44.78 45.42 48.17	46.12	
III	Al	64.72 65.55 64.32	64.86	Al_2Cu
	Cu	28.46 33.64 32.88	31.66	

3.2. Mechanical Properties

Uniaxial tensile tests were conducted at room temperature to investigate the impact of overall thickness and the copper thickness ratio of Cu/Al/Cu composites on their mechanical properties. Figure 5 illustrates the true stress–strain curves for Cu/Al/Cu composites across various overall thicknesses and copper thickness ratios. As depicted in Figure 5, Cu/Al/Cu composites with differing overall thicknesses and copper thickness ratios exhibit distinct tensile properties. For the 1 mm Cu/Al/Cu composite with copper thickness ratios of 20% and 35% ("1-20" and "1-35"), a significant enhancement in both ultimate tensile strength (UTS) and elongation is observed when the copper thickness ratio is increased from 20% to 35%. The yield strength and ultimate tensile strength for the "1-35" Cu/Al/Cu composite are approximately 61 MPa and 128 MPa, respectively. This improvement is attributed solely to the additional bearing capacity provided by the interface's intermittent distributions of intermetallic compounds (IMCs) in the Cu/Al/Cu composite with a 35% copper thickness ratio. The 2 mm Cu/Al/Cu composites demonstrate a similar trend, with ultimate tensile strength and elongation values for the "2-20" and "2-35" composites being around 101.7 MPa and 13.1%, and 134.7 MPa and 18.2%, respectively. Finally, for the Cu/Al/Cu composites with a 35% copper thickness ratio at varying thicknesses ("1-35", "2-35", and "4-35"), a slight increase in tensile strength and a decrease in elongation are observed when the thickness is increased from 1 mm to 2 mm. However, increasing the thickness to 4 mm results in a decrease in tensile strength and a significant improvement in elongation. This minor mechanical variation is attributed to the characteristics of the IMCs'

distribution at the interface of the Cu/Al/Cu composites with different thicknesses. The 4 mm-thick composites with a 35% Cu ratio exhibit a regular intermittent IMC distribution with larger gap distances, allowing the Cu and Al layers to extrude and fill these gaps, which facilitates synergistic deformation during the tensile process.

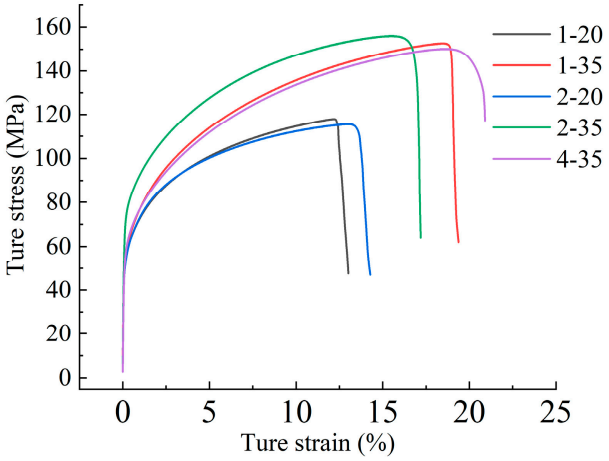


Figure 5. True stress–strain curves of Cu/Al/Cu composites with varying overall thicknesses and copper thickness ratios.

Additionally, Kocks–Mecking (K-M) plots [33], derived from true stress–strain curves, were utilized to assess strain-hardening behavior. It is important to note that only the stress increment (σ-σ_y) and strain-hardening rate ($\theta = d\sigma/d\varepsilon$) during the plastic deformation stage were considered, where σ_y represents the yield stress. The K-M plots in Figure 6b,c display an approximately linear region, referred to as stage III; the slope in this stage correlates with the dynamic recovery rate. The Cu/Al/Cu composites with higher Cu thickness ratios demonstrated a lower dynamic recovery rate compared to other conditions, suggesting a greater strain-hardening capacity. This tensile behavior is attributed to the intermittent interface distribution of intermetallic compounds in the Cu/Al/Cu composites with higher Cu thickness ratios, which enhances mechanical bonding at the joint interface. As illustrated in Figure 6c, as the overall thickness of the composite with 20% Cu ratio increased from 1 mm to 2 mm, the differences between the curve slopes become less pronounced compared to those with varying Cu thickness ratios; Thus, their dynamic recovery behavior and strain-hardening properties are nearly similar. However, for the composite with a 35% Cu thickness ratio, the strain hardening rate was greater with increased thickness during the initial stage of uniform plastic deformation.

Figure 7 displays the comparison of yield strength, ultimate tensile strength, and elongation-to-failure of the fabricated Cu/Al/Cu composites with different overall thicknesses and copper thickness ratios. It is evident that both ultimate tensile strength and elongation improved with an increasing Cu thickness ratio. Specifically, for the 1 mm and 2 mm Cu/Al/Cu composites, when the Cu thickness ratio increased from 20% to 35%, ultimate tensile strength (UTS) and elongation improved by approximately 22.3% and 70.9%, and 32.4% and 38.7%, respectively. Further, yield strength increased with an increasing Cu thickness ratio for both the 1 mm and 2 mm Cu/Al/Cu composites. This variation in mechanical properties is likely related to the fragmentation of the intermetallic compounds in Cu/Al/Cu composites with higher Cu thickness ratios, as the produced IMCs (Al_4Cu_9, AlCu, and Al_2Cu) tend to be hard and brittle. This fracture distribution of IMCs provides additional mechanical bonding compared to a continuous IMC distribution and enhances the UTS. Conversely, as the thickness of Cu/Al/Cu composites increased from 1 mm to 2 mm, the ultimate tensile strength increased and elongation decreased. Upon

further increasing the overall thickness to 4 mm, the ultimate tensile strength decreased from 134.7 MPa to 126.1 MPa, representing a 6% decline. In contrast, elongation increased by 19%, rising from 18.2% to 21.2%.

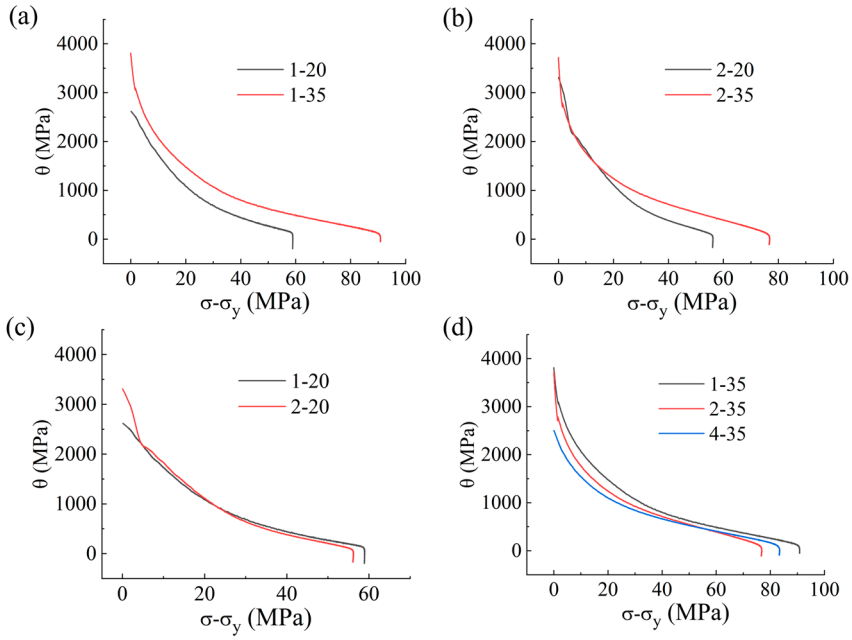


Figure 6. Kocks–Mecking (K-M) plots for the Cu/Al/Cu trilayer composites for various overall thicknesses and copper thickness ratios: (**a**) comparison between "1-20" and "1-35", (**b**) comparison between "2-20" and "2-35", (**c**) comparison between "1-20" and "2-20", and (**d**) comparison between "1-35", "2-35", and "4-35".

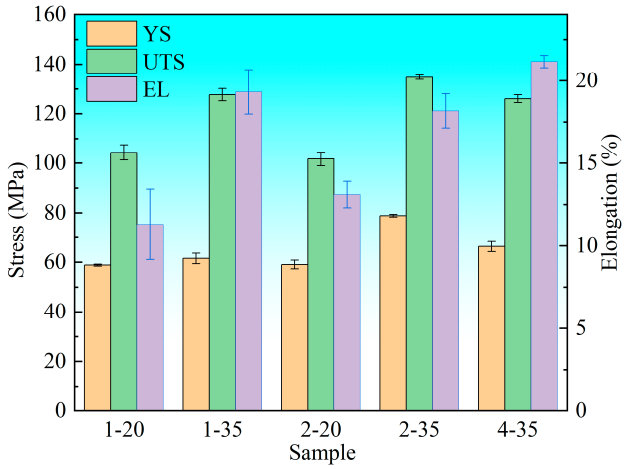


Figure 7. Yield strength, ultimate tensile strength, and elongation of the Cu/Al/Cu composites with varying overall thicknesses and copper thickness ratios.

3.3. Fractography

Figure 8 illustrates the fracture morphology of Cu/Al/Cu composites under various conditions after conducting a tensile test at room temperature. It is clear that all composites experienced significant plastic deformation following tensile loading, with cracks forming at the Cu/Al interface. During the tensile process, the interface was compromised due to shear stress resulting from the differing mechanical properties of the copper and aluminum layers. Gaps also emerged between the Cu and Al layers, indicating mutual sliding during deformation. As depicted in Figure 8a,b, the interface gap between the Cu and Al layers in the "1-35" composite was tighter compared to the "1-20" counterpart, suggesting

more coordinated deformation in Cu/Al/Cu composites with higher Cu thickness ratios. Additionally, the fracture microstructure of the "1-20" composite exhibited delamination at the Cu/Al interface, along with tear ridges on the fracture surface of the Al side. In contrast, the fracture morphology of the "1-35" composite displayed dimples on the Al side, which are characteristic of ductile fractures and were absent in the "1-20" composites. Moreover, the Cu layer in the "1-35" composite showed more pronounced tear ridges than its "1-20" counterpart, indicating a greater degree of deformation in the Cu layer. This fracture behavior in Cu/Al/Cu composites with varying overall thicknesses and Cu thickness ratios aligns well with the tensile test results discussed previously. As shown in Figure 8c,d, when the overall thickness increased to 2 mm, the fracture interface became more compact and exhibited fewer interface cracks with an increased Cu thickness ratio, suggesting improved interface bonding. Similarly, the Al layer in the "2-35" composite displayed denser and deeper dimples compared to the "2-20" counterpart. In conclusion, for composites with the same overall thickness, increasing the Cu thickness ratio from 20% to 35% facilitates more effective co-deformation between the Cu and Al layers, and ductile fracture characteristics became more apparent. This phenomenon may be attributed to the differing interface microstructures and the dispersed fracture of intermetallic compounds in Cu/Al/Cu composites with higher Cu thickness ratios, which can accommodate greater plastic strains and enhance coordinated deformation.

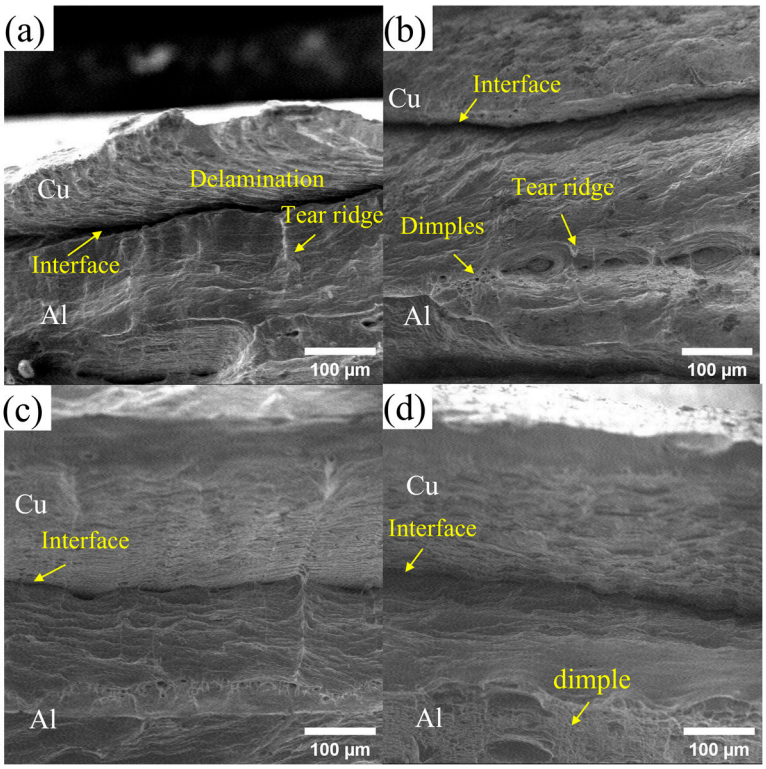


Figure 8. Fracture morphology of Cu/Al/Cu composites with varying overall thicknesses and copper thickness ratios after undergoing tensile testing at room temperature: (**a**) "1-20", (**b**) "1-35", (**c**) "2-20", and (**d**) "2-35".

Figure 9 illustrates the fracture morphology of the interface in Cu/Al/Cu composites with varying overall thicknesses and copper thickness ratios. As shown in Figure 9a, the Al side of the "1-35" composite has clear tear ridges, which means that the fracture is ductile. The Cu layer, on the other hand, has a relatively smooth fracture. In the case of the "2-35" composite depicted in Figure 9b, the tear ridge features in the Al layer become less pronounced as the overall thickness increases; however, some shear dimples appear,

suggesting a different deformation behavior during tensile loading. Additionally, there are residual bonding areas at the Cu/Al fracture interface of the "2-35" composite. For the "4-35" composite presented in Figure 9c, the fracture morphology in the Cu layer appears rougher compared to its thinner counterparts, while the Al layer exhibits fractures characterized by dimples and tear ridges. The 2 mm Cu/Al/Cu composites with a 35% Cu thickness ratio demonstrate well-coordinated deformation between the Cu and Al layers. Furthermore, for the Cu/Al/Cu composites with a 20% Cu thickness ratio shown in Figure 9d,e, as the overall thickness increases, the interface fracture becomes tighter, and the Cu layer fracture presents a tilted surface. This indicates coordinated deformation in the "2-20" composite compared to the "1-20" counterpart, which is consistent with the improved elongation-to-failure observed in the "2-20" composite.

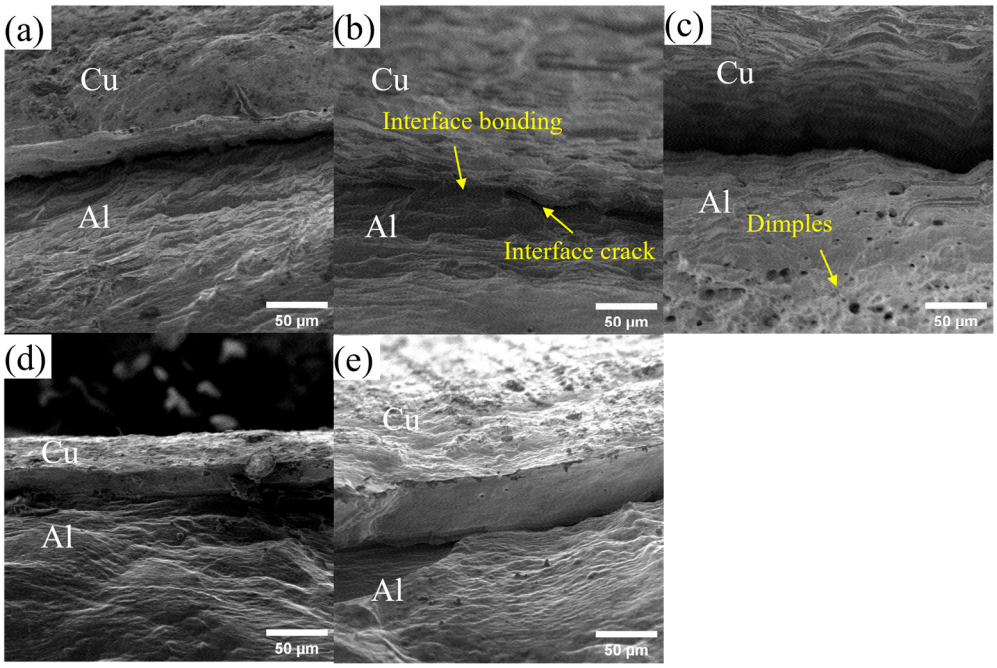


Figure 9. Fracture morphology of the interface in the Cu/Al/Cu composites with varying overall thicknesses and copper thickness ratios after undergoing tensile testing at room temperature: (**a**) "1-35", (**b**) "2-35", (**c**) "4-35", (**d**) "1-20", and (**e**) "2-20".

4. Conclusions

In this study, we comprehensively examined the interfacial microstructure, mechanical properties, and fracture mechanisms of Cu/Al/Cu trilayered composites with varying overall thicknesses and copper thickness ratios. The distribution of intermetallic compounds varied with overall thickness and copper thickness ratio, leading to distinct mechanical properties and fracture mechanisms. These findings offer practical methods and valuable guidelines for enhancing the interface bonding strength of Cu/Al/Cu composites. The key conclusions are summarized as follows:

(1) The Cu/Al/Cu composites with varying Cu thickness ratios exhibited distinct interfacial microstructures and IMC distributions. For both 1 mm and 2 mm composites, an increase in the Cu thickness ratio from 20% to 35% resulted in an IMC distribution shift from a continuous pattern to intermittent fragments. This change in the distribution of IMCs suggested that higher Cu thickness ratios contribute to additional mechanical bonding at the Cu/Al interface, potentially due to increased bonding strength at the interface.

(2) The increase in the copper thickness ratio of Cu/Al/Cu composites has led to improvements in both tensile strength and elongation. Specifically, for the 1 mm composite,

increasing the Cu thickness ratio from 20% to 35% results in enhancements of approximately 22% in UTS and 71% in elongation. In contrast, the 2 mm composite shows increase of 32% in UTS and 39% in elongation when the Cu thickness ratio is raised from 20% to 35%.

(3) For Cu/Al/Cu composites with a 35% copper thickness ratio, changes in the overall thickness of the composite affect its mechanical properties. There was a slight decrease in ultimate tensile strength as the overall thickness increased from 1 mm to 3 mm. Initially, the elongation decreased slightly, then increased, reaching a maximum value of 21.2% at a thickness of 4 mm.

(4) The fractography of Cu/Al/Cu composites with varying overall thicknesses and Cu thickness ratios demonstrated distinct fracture mechanisms. When the Cu thickness ratio was 20%, the Al layer exhibited ductile fracture characteristics, characterized by dense and deep dimples, while the Cu layer also displayed a ductile fracture mode, marked by tear ridges. As the Cu thickness ratio increased, the fracture interface became more compact, resulting in a greater number of dimples observed in the Al layer. Furthermore, the bonding interface showed improved compactness, indicating enhanced mechanical strength and elongation, as confirmed by tensile tests.

Author Contributions: Conceptualization, W.B. and M.E.; Methodology, H.C. and Y.Z.; Software, N.Z. Validation, Q.W., W.B. and M.E.; Formal analysis, Q.W., W.B. and M.E.; Funding acquisition, Q.W.; Investigation, H.C., N.Z. and Y.Z.; Visualization, Y.Z. and N.Z.; Data curation, Q.W., W.B. and M.E.; Project administration, Q.W.; Resources, Q.W. and W.B.; Supervision, Q.W.; Writing—original draft, Q.W., W.B. and M.E.; Writing—review and& editing, Q.W., W.B., H.C. and M.E. All authors have read and agreed to the published version of the manuscript.

Funding: This work was financially supported by the National Key Research and Development Program of China (Grant Nos. 2021YFB3701303 and 2024YFB3714303), the National Natural Science Foundation of China (No. U1902220), and the SJTU-Warwick Joint Seed Fund (Nos. SJTU2210 and SJTU2024).

Data Availability Statement: All data generated or analyzed during this study are included in this published article.

Conflicts of Interest: The authors declare no conflicts of interest.

References

1. Ren, Z.; Gao, X.; Hou, J.; Huang, Z.; Wang, T.; Huang, Q.; Liu, X. Achieving Excellent Strength-Elongation Synergy in Corrugated Cu/Al Laminated Composites by Flat Finish Roll Bonding. *J. Alloys Compd.* **2024**, *982*, 173782. [CrossRef]
2. Ebrahimi, M.; Liu, G.; Li, C.; Wang, Q.; Jiang, H.; Ding, W.; Su, F.; Shang, Z. Characteristic Investigation of Trilayered Cu/Al8011/Al1060 Composite: Interface Morphology, Microstructure, and in-Situ Tensile Deformation. *Prog. Nat. Sci. Mater. Int.* **2021**, *31*, 679–687. [CrossRef]
3. Ebrahimi, M.; Liu, G.; Li, C.; Wang, Q.; Jiang, H.; Ding, W.; Su, F. Experimental and Numerical Analysis of Cu/Al8011/Al1060 Trilayered Composite: A Comprehensive Study. *J. Mater. Res. Technol.* **2020**, *9*, 14695–14707. [CrossRef]
4. Cai, H.; Yang, S.; Li, J.; Wang, Q.; Zhao, Y.; Jia, Q.; Ebrahimi, M.; Liu, L.; Guo, F. Growth Behavior of Intermetallics with Discontinuous Distribution of Cu/Al/Cu Trilayered Composites during Annealing. *J. Mater. Res. Technol.* **2026**, *42*, 2596–2607. [CrossRef]
5. Song, H.; Hao, W.; Mu, X.; Han, T.; Che, C.; Geng, G. Effect of Pulse Current-Assisted Rolling on the Interface Bonding Strength and Microstructure of Cu/Al Laminated Composite. *Metals* **2020**, *10*, 1555. [CrossRef]
6. Chen, D.; Zhang, H.; Li, H.; Zhu, R.; Zhu, Y.; Jiang, Z. Study on Microstructure and Properties of Ultra-Thin Cu/Al Composite Sheets Using the Cold-Rolled Composite Method at the Microscale. *Metals* **2023**, *13*, 780. [CrossRef]
7. Niu, H.; Gao, X.; Jiang, L.; Han, J.; Liu, P.; Wang, T. Research on Bonding Mechanism of Cu/Al Corrugated Composite Plates Rolled by Flat Finish Roll Bonding. *Mater. Today Commun.* **2024**, *40*, 109303. [CrossRef]
8. Yamashita, M.; Iwatsuka, T.; Taguchi, H.; Nikawa, M. Impact Joining of Pure Copper C1100 and Aluminum Alloy A6061-T6 Plates at Edges. *Metals* **2022**, *12*, 1565. [CrossRef]

9. Liu, W.; Wang, X.; Zhang, J.; Zhang, G.; Liu, P. Al-Clad Cu Bond Wires for Power Electronics Packaging: Microstructure Evolution, Mechanical Performance, and Molecular Dynamics Simulation of Diffusion Behaviors. *Mater. Today Commun.* **2024**, *41*, 110940. [CrossRef]
10. Ebrahimi, M.; Liu, G.; Wang, Q.; Jiang, H.; Ding, W.; Shang, Z.; Luo, L. Evaluation of Interface Structure and High-Temperature Tensile Behavior in Cu/Al8011/Al5052 Trilayered Composite. *Mater. Sci. Eng. A* **2020**, *798*, 140129. [CrossRef]
11. Zhao, Y.; Ebrahimi, M.; Wu, L.; Attarilar, S.; Wang, Q. Tailored Annealing for Interfacial Design and Mechanical Optimization of Cu18150/Al1060/Cu18150 Trilayer Composites. *Metals* **2026**, *16*, 176. [CrossRef]
12. Hoseini Athar, M.M.; Tolaminejad, B. Weldability Window and the Effect of Interface Morphology on the Properties of Al/Cu/Al Laminated Composites Fabricated by Explosive Welding. *Mater. Des.* **2015**, *86*, 516–525. [CrossRef]
13. Chang, Q.; Xie, J.; Mao, A.; Wang, W. Study on Interface Structure of Cu/Al Clad Plates by Roll Casting. *Metals* **2018**, *8*, 770. [CrossRef]
14. Sonti, K.S.M.; Dash, B.; Vamsi, K.V.; Bandyopadhyay, H.; Ravisankar, B.; Sivaprasad, K.; Karthikeyan, S. Deformation Behavior of Al/Cu in-Situ Metal-Intermetallic Laminates at Low and High Strain Rates. *J. Alloys Compd.* **2021**, *873*, 159767. [CrossRef]
15. Standley, M.R.; Knezevic, M. Towards Manufacturing of Ultrafine-Laminated Structures in Metallic Tubes by Accumulative Extrusion Bonding. *Metals* **2021**, *11*, 389. [CrossRef]
16. Zheng, H.; Zhang, R.; Xu, Q.; Kong, X.; Sun, W.; Fu, Y.; Wu, M.; Liu, K. Fabrication of Cu/Al/Cu Laminated Composites Reinforced with Graphene by Hot Pressing and Evaluation of Their Electrical Conductivity. *Materials* **2023**, *16*, 622. [CrossRef] [PubMed]
17. Park, S.; Joo, Y.; Kang, M. Effect of Backing Plate Materials in Micro-Friction Stir Butt Welding of Dissimilar AA6061-T6 and AA5052-H32 Aluminum Alloys. *Metals* **2020**, *10*, 933. [CrossRef]
18. Mao, Y.; Ni, Y.; Xiao, X.; Qin, D.; Fu, L. Microstructural Characterization and Mechanical Properties of Micro Friction Stir Welded Dissimilar Al/Cu Ultra-Thin Sheets. *J. Manuf. Process.* **2020**, *60*, 356–365. [CrossRef]
19. Magalhães, D.C.C.; Cintho, O.M.; Sordi, V.L.; Kliauga, A. Improved Tensile Properties in Heterostructured 1050/7050 Al Sheets Produced by Accumulative Roll Bonding. *J. Mater. Res. Technol.* **2022**, *17*, 2014–2025. [CrossRef]
20. Xu, R.; Liang, N.; Zhuang, L.; Wei, D.; Zhao, Y. Microstructure and Mechanical Behaviors of Al/Cu Laminated Composites Fabricated by Accumulative Roll Bonding and Intermediate Annealing. *Mater. Sci. Eng. A* **2022**, *832*, 142510. [CrossRef]
21. Ran, M.; Bian, G.; Zhang, H.; Yan, J.; Wang, W. Electropulsing-Enhanced Atomic Diffusion and Recrystallization to Optimize Mechanical Properties of Al/Cu Laminated Metal Composites. *J. Manuf. Process.* **2024**, *119*, 224–234. [CrossRef]
22. Lei, J.; Ma, L.; Cai, Z.; Jia, W.; Zhi, C.; Yuan, Y.; Pan, H.; Xie, H. Interfacial Fracture Characteristics of Mg/Al Composite Plates with Different Thickness Ratios by Asymmetrical Rolling with Differential Temperature Rolls. *Mater. Sci. Eng. A* **2023**, *869*, 144764. [CrossRef]
23. Qin, D.; Chen, C. Failure Behavior and Mechanical Properties of Novel Dieless Clinched Joints with Different Sheet Thickness Ratios. *J. Cent. S. Univ.* **2022**, *29*, 3077–3087. [CrossRef]
24. Zou, X.; Liu, T.; Liu, W.; Wang, F.; Li, Y.; Su, R.; Shi, L. The Effect of Cu on Microstructure, Mechanical Properties and Fracture Behavior of Al-15 %Mg_2Si Composite. *J. Alloys Compd.* **2025**, *1012*, 178497. [CrossRef]
25. Yan, T.; Zhang, L.; Yuan, X.; Li, B.; Bai, J.; Fu, H.; Zhang, H.; Zhang, H. Simultaneous Enhancement of Tensile Properties and Fracture Toughness of Bulk Metallic Glass Composites. *Acta Mater.* **2025**, *291*, 121018. [CrossRef]
26. Li, S.; Yuan, J.; Liu, W.; Hao, P.; Xu, S.; Yao, J.; Fan, Q.; Yang, L. Underlying Toughening Mechanisms of TB9/TC4 Laminated Composite Suffering Impact Load. *J. Alloys Compd.* **2025**, *1022*, 179872. [CrossRef]
27. Lei, J.; Ma, L.; Cai, Z.; Jia, W.; Yuan, Y.; Pan, H.; Xie, H. Interfacial Microstructure Evolution for Coordinated Deformation of Mg/Al Composite Plates by Asymmetrical Rolling with Differential Temperature Rolls. *J. Magnes. Alloys* **2024**, *12*, 4244–4258. [CrossRef]
28. Atifeh, S.M.; Hashemi, R.; Sedighi, M. Investigation and Optimization on the Formability of Aluminum 1050/Stainless Steel 304L Bilayer Sheets Fabricated by Cold Roll Bonding Considering the Box-Behnken Method. *J. Mater. Res. Technol.* **2024**, *31*, 3453–3465. [CrossRef]
29. Cheng, Y.; Liu, W.; Wang, T.; Li, T.; Huang, Q. Study on the Effects of Initial Temperature and Thickness Ratio of Component Metals on the Preparation of Aluminum/Steel Clad Plates by the New Different Temperature Rolling Method. *J. Manuf. Process.* **2023**, *95*, 229–241. [CrossRef]
30. Xia, Y.; Wu, H.; Miao, K.; Li, X.; Xu, C.; Geng, L.; Xie, H.; Fan, G. Effects of the Layer Thickness Ratio on the Enhanced Ductility of Laminated Aluminum. *J. Mater. Sci. Technol.* **2022**, *111*, 256–267. [CrossRef]
31. Wang, Z.; Bian, Y.; Yang, M.; Ma, R.; Fan, Y.; Du, A.; Zhao, X.; Cao, X. Investigation of Coordinated Behavior of Deformation at the Interface of Cu–Al Laminated Composite. *J. Mater. Res. Technol.* **2023**, *24*, 6545–6557. [CrossRef]
32. Shen, C.; Wang, C.; Wei, X.; Li, Y.; van der Zwaag, S.; Xu, W. Physical Metallurgy-Guided Machine Learning and Artificial Intelligent Design of Ultrahigh-Strength Stainless Steel. *Acta Mater.* **2019**, *179*, 201–214. [CrossRef]

33. Wang, C.; Zhang, Z.; Jing, X.; Yang, Z.; Xu, W. Optimization of Multistage Femtosecond Laser Drilling Process Using Machine Learning Coupled with Molecular Dynamics. *Opt. Laser Technol.* **2022**, *156*, 108442. [CrossRef]
34. Zhang, Z.; Liu, S.; Zhang, Y.; Wang, C.; Zhang, S.; Yang, Z.; Xu, W. Optimization of Low-Power Femtosecond Laser Trepan Drilling by Machine Learning and a High-Throughput Multi-Objective Genetic Algorithm. *Opt. Laser Technol.* **2022**, *148*, 107688. [CrossRef]
35. Xie, W.-T.; Song, D.-N.; Tang, W.-C.; Ma, J.-W.; Li, J.-H. Auxiliary Support Path Planning for Robot-Assisted Machining of Thin-Walled Parts with Non-Uniform Thickness and Closed Cross-Section Based on a Neutral Surface. *J. Manuf. Process.* **2025**, *147*, 16–28. [CrossRef]
36. Zhang, G.; Gu, J.; Shi, H.; Zhang, P.; Yu, Z.; Zhao, W.; Yuan, X.; Zhang, L.; Yang, G. Microstructures and Mechanical Properties Analysis of TiAl Joints Using Novel Brazing Filler Metal. *Weld. World* **2026**, *70*, 2237–2251. [CrossRef]
37. Xu, X.; Zhou, S.; Li, B.; Wei, Y.; Wang, H. Investigation Interfacial Wetting Behavior of Copper Matte/Slag/Fe_3O_4 Enriched Intermediate Layer During High Temperature Smelting. *Metall. Mater. Trans. B* **2025**, *56*, 449–471. [CrossRef]
38. Meng, X.; Wang, W.; Xie, Y.; Wang, N.; Ma, X.; Dong, J.; Gao, J.; Yang, T.; Huang, Y. Microstructural Modification and Stress Corrosion Mechanisms of In-Situ Rolling Friction Stir Welding Joints. *Mater. Charact.* **2026**, *231*, 115884. [CrossRef]
39. Gai, J.; Yang, X.; Zhao, Y. Electroacoustic Wave Scattering from Cylindrical Inhomogeneities in Transversely Isotropic Piezoelectric Composites. *Mater. Des.* **2026**, *261*, 115296. [CrossRef]
40. Hu, Y.; Chen, J.; Zhen, Y.; Han, Y.; Yu, C.; Xiong, K.; Zhang, S. Study on the Wettability, Intermetallic Compound Growth, Voids Formation and Mechanical Properties of Cu/Sn Joints with Changes in Substrate Roughness for Electronic Packaging. *J. Mater. Sci. Mater. Electron.* **2025**, *36*, 851. [CrossRef]
41. Hong, Y.; Dong, D.D.; Zou, G.P.; Li, Y.; Lin, S.S.; Kuang, T.C.; Wu, Y.Z.; Dai, M.J. The Corrosion Response of the Heterogeneous Nitriding Structure Originated from the Laser Additive Manufactured Steel. *Corros. Sci.* **2023**, *218*, 111188. [CrossRef]
42. Wei, J.; Han, J.; Jia, Y.; Wang, T.; Huang, Q. Evolution of Multiscale Heterostructures and Comprehensive Properties Improvement in the Large Thickness Ratio Ti/Al/Mg Clad Plates under Heterothermal Rolling. *J. Magnes. Alloys* **2026**, *18*, 101863. [CrossRef]
43. Zhang, Z.; Wan, L.; Yang, Y.; Feng, Z.; Shi, Y. Enhancing Interlayer Bonding and Tensile Isotropy in Additive Friction Stir Deposition of Al-Zn-Mg-Cu Alloys via a Novel Tool Design Strategy. *Addit. Manuf.* **2026**, *125*, 105250. [CrossRef]
44. Chang, D.; Wang, P.; Zhao, Y. Effects of Asymmetry and Annealing on Interfacial Microstructure and Mechanical Properties of Cu/Al Laminated Composite Fabricated by Asymmetrical Roll Bonding. *J. Alloys Compd.* **2020**, *815*, 152453. [CrossRef]
45. Mao, Z.; Xie, J.; Wang, A.; Wang, W.; Ma, D.; Liu, P. Effects of Annealing Temperature on the Interfacial Microstructure and Bonding Strength of Cu/Al Clad Sheets Produced by Twin-Roll Casting and Rolling. *J. Mater. Process. Technol.* **2020**, *285*, 116804. [CrossRef]
46. Wang, B.; You, B.; Hu, Y.; Fu, L.; Yu, C.; Xiao, H. Improvement of Bonding Behavior of Cold-Rolled Stainless Steel/Copper Composite Plates via Surface Spinel Structure Treatment. *J. Mater. Res. Technol.* **2025**, *35*, 1586–1595. [CrossRef]
47. Qiu, J.; Li, Y.; Liu, W.; Zhou, H.; Cao, C.; Bi, G. Rolling In-Situ Generation of Metallurgical and Mechanical Bonding Improves Mechanical Properties and Synergistic Deformation Ability of Semi-Solid Cast-Rolled Aluminum/Steel Composite Plate. *J. Mater. Process. Technol.* **2025**, *339*, 118821. [CrossRef]
48. Cai, H.; Yang, S.; Wang, Q.; Zhao, Y.; Jia, Q.; Ebrahimi, M.; Liu, L.; Guo, F.; Shang, Z. Interfacial Shear Fracture Behavior of C18150Cu/1060Al/C18150Cu Trilayered Composite at Different Temperatures. *Materials* **2025**, *18*, 559. [CrossRef] [PubMed]
49. Deng, Z.; Xiao, H.; Yu, C. Effect of Intermetallic Compounds Distribution on Bonding Strength of Steel–Aluminum Laminates. *Mater. Des.* **2022**, *222*, 111106. [CrossRef]
50. Zhang, S.; Cai, L.; Nguyen, T.A.N.; Geng, M.; Gao, K.; Hong, S.-T.; Kim, M.-J. Effects of Intermetallic Evolution by Electrically Assisted Rapid Heat Treatment on the Mechanical Performance and Formability of Aluminum Clad Steel. *Int. J. Precis. Eng. Manuf. Technol.* **2023**, *10*, 367–379. [CrossRef]
51. Cai, H.; Wang, Q.; Zhang, N.; Ebrahimi, M.; Zhao, Y.; Liu, L.; Guo, F. Shear Behavior of Cu/Al/Cu Trilayered Composites Prepared by High-Temperature Oxygen-Free Rolling. *J. Alloys Compd.* **2024**, *1004*, 175857. [CrossRef]

Disclaimer/Publisher's Note: The statements, opinions and data contained in all publications are solely those of the individual author(s) and contributor(s) and not of MDPI and/or the editor(s). MDPI and/or the editor(s) disclaim responsibility for any injury to people or property resulting from any ideas, methods, instructions or products referred to in the content.